

Effects of different Form-factors in Meson-Photon-Photon Transitions and the Muon Anomalous Magnetic Moment¹

Johan Bijnens and Fredrik Persson

*Department of Theoretical Physics, Lund University,
Sölvegatan 14A, S22362 Lund, Sweden*

Abstract

The exact form of the form-factor associated with a meson-photon-photon vertex is not known. Different suggestions exist, based on constraints from QCD and on recent experiments. Four different form-factors are studied in this article.

We calculate decay rates for the decays $\pi^0 \rightarrow \gamma\gamma$, $\eta \rightarrow \gamma e^+e^-$, $\eta \rightarrow \mu^+\mu^- e^+e^-$ and $\eta \rightarrow e^+e^- e^+e^-$ and cross sections for the processes $e^+e^- \rightarrow PS e^+e^-$, where $PS = \pi^0, \eta$ or η' . The results depend on the choice of form-factor and we examine if the differences are large enough to distinguish in upcoming experiments.

The dominant part of the light-by-light contribution to the muon anomalous magnetic moment is also calculated. Here the uncertainty around the choice of form-factor implies that it is possible to estimate a smallest error in the theoretical value of this contribution.

¹Master of Science Thesis by Fredrik Persson with thesis advisor: Johan Bijnens. A more paper like version with more references will follow.

1 Introduction

Understanding the structure of the natural universe can be seen as a three-part problem. Identifying the basic particles that are the constituents of matter, knowing what forces they feel and knowing how to calculate the behaviour of the particles given the forces. The Standard Model is the theory that tries to answer these questions today.

The particles can be put into two categories, matter particles and gauge bosons. The matter particles, the quarks and the leptons, are the building blocks of nature. Both are spin-1/2 fermions but the quarks also have colour charge as described in QCD. So far there are known to exist six kinds of quarks and six kinds of leptons.

The quarks are called up, down, strange, charm, top and bottom. They are denoted by their first letter and are divided into three doublets, called generations:

$$\begin{pmatrix} u \\ d \end{pmatrix} \quad \begin{pmatrix} c \\ s \end{pmatrix} \quad \begin{pmatrix} t \\ b \end{pmatrix}.$$

The top row has electric charge $q = +(2/3)e$ and the bottom row has $q = -(1/3)e$, where e is the magnitude of the electron's charge.

The six leptons are also arranged in three generations:

$$\begin{pmatrix} \nu_e \\ e \end{pmatrix} \quad \begin{pmatrix} \nu_\mu \\ \mu \end{pmatrix} \quad \begin{pmatrix} \nu_\tau \\ \tau \end{pmatrix}.$$

The electron, muon and tau have electric charge $-e$ and each has its own neutrino of electric charge zero. The quarks and the leptons are the basic particles of matter.

The second type of particles are the gauge bosons, which all have integer spin. They are best described together with the forces. Classically, a force is seen as a field, e.g. a charged object is surrounded by an electric field. But in Quantum Field Theory, which is based on special relativity and quantum mechanics, an important part is that particles and fields are treated in the same way. Whether they behave as particles or fields depend on the circumstances and the gauge bosons are just those particles that correspond to the forces and their fields. There are four forces in nature and each has its own gauge bosons:

<u>Force</u>	<u>Acts on</u>	<u>Gauge bosons</u>
gravitation	all particles	graviton
electromagnetic	all electrically charged particles	γ
weak	quarks, leptons electroweak gauge bosons	W^+ , W^- , Z^0
strong	all coloured particles	g_i , $i = 1 \dots 8$

The gravitational force acts upon all particles but the strength depends on the mass and it can be disregarded in all but the highest energy calculations in particle physics. The electromagnetic force affects charged objects and holds e.g. the electrons and the nuclei together in atoms. It is transmitted by the photons. The weak interaction, or force, is

needed to explain e.g. the β -decay of nuclei and it is transmitted by three very heavy bosons, which makes it a short-range interaction according to Heisenbergs uncertainty relation. The strong force holds the quarks together inside the nucleons as well as the protons and neutrons inside nuclei. The carriers are the eight gluons which themselves have colour charge.

Furthermore, all particles, fermions and bosons, have antiparticles. They have opposite values of all charges, but the same mass. [1, 2]

Particles with colour charge like the quarks and gluons can't exist on their own. They are permanently bound inside colourless hadrons. Hadrons can be baryons, in which case they are made up of three quarks, or mesons, if they are made up of one quark and one anti-quark. Depending on how they behave under parity-transformations and rotations, the mesons can be scalar-mesons, vector-mesons etc. We study properties of the three pseudo-scalar mesons π^0 , η and η' in this article.

1.1 Form-factors

An interesting thing to keep in mind is that the known universe is made up of u-quarks, d-quarks, electrons, ν_e and the gauge bosons. All the other quarks and leptons existed at an early stage of the universe and can today only be seen in cosmic rays and accelerator experiments. Such experiments makes it possible to study the properties of the different interactions, i.e. how the particles behave given the forces.

For example, studying $\gamma\gamma$ scattering provides a unique opportunity to learn the properties of strong interactions. Although in $\gamma\gamma$ scattering the probe and the target are both photons that are carriers of the electromagnetic force, they can produce a pair of quarks that interact strongly and are observed in the form of hadrons, e.g. pseudo-scalar mesons. However, the transition between a meson and two photons can't be calculated from QCD directly. Therefore, a temporary solution is to calculate the process without including all effects of the quarks and gluons and at the end take the neglected effects into account with an extra factor. This factor is, for historical reasons, known as a form-factor. The shape of this form-factor is however not known exactly. There exist different educated guesses which fits certain demands from QCD, but since one doesn't know exactly which one to use it is important to know which effects a specific choice will have. This article studies the variation of some physical quantities with the choice of form-factor.

The article is organized as follows. In section 2 the form-factors are presented in more detail. Section 3 includes a comparison between the decay-rates for different form-factors for processes involving η . Section 4 treats the cross-section of $e^+e^- \rightarrow e^+e^-PS$, where PS is π^0 , η or η' , and how it is affected by the choice of form-factor. Section 5 contains a discussion of the effect the form-factors have on the theoretic value of the muon anomalous magnetic moment and section 6 is a summary of this article.

2 Form-factors in Meson-Photon-Photon Transitions

The transition between a meson and two photons is very hard to calculate in QCD. That depends on the fact that for low energies α_s , the strong coupling constant, is too large for a perturbative approach to work. Beside perturbative calculations no good method exist in this case so the problem gets complicated and approximations have to be made.

In the approximation that the quarks are massless, QCD has chiral symmetry. That means that all quarks, right-handed as well as left-handed, are treated in the same way and give the same results². According to Noether's theorem, which states;

For a system described by a Lagrangian, any continuous symmetry which leaves invariant the action, $\int \mathcal{L} dt$, leads to the existence of a conserved current,

this implies that the current, S^μ , which corresponds to the chiral symmetry, fulfills the relation

$$\partial_\mu S^\mu = 0.$$

But when one combines QCD and electromagnetism, as in the vertex we are studying, this is no longer true. The four-divergence of the current isn't zero anymore but instead it has the form

$$\partial_\mu S^\mu = C e^2 \varepsilon^{\mu\nu\alpha\beta} F_{\mu\nu}^\gamma F_{\alpha\beta}^\gamma,$$

where C is a known constant, e the magnitude of the electron's charge, $\varepsilon^{\mu\nu\alpha\beta}$ the totally antisymmetric Levi-Civita tensor and F^γ the electromagnetic field strength.

This was very surprising to the people that first calculated it so it was given the name 'the anomaly'. But since this effect exists the effective Lagrangian that should describe this vertex should reproduce it. That puts strong constraints on how the Lagrangian can look and there is actually only one way to construct it so that it fulfills this anomaly condition. From this Lagrangian, the term which describes the low-energy processes that include π^0 , η or η' and two photons can be written

$$\mathcal{L} = -\frac{e^2}{4\sqrt{2}\pi^2 F_\pi} \partial_\mu A_\nu(x) A_\alpha(x) \partial_\beta \phi(x) \varepsilon^{\mu\nu\alpha\beta},$$

where F_π is the pion decay constant, $A_\nu(x)$ and $A_\alpha(x)$ the photon fields and $\phi(x)$ the pseudo-scalar field.

However, this Lagrangian only describes the process in the limit where the pseudo-scalar is seen as a point-like particle, with no inner structure, and the reaction is seen as in Fig. 1. In reality, these particles are not pointlike but instead made up of quarks and

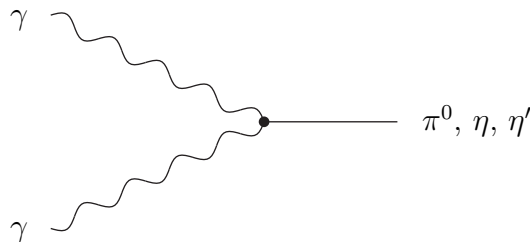


Figure 1: Feynman diagram for the transition when the reaction is seen as pointlike.

²In reality, this symmetry is spontaneously broken[3].

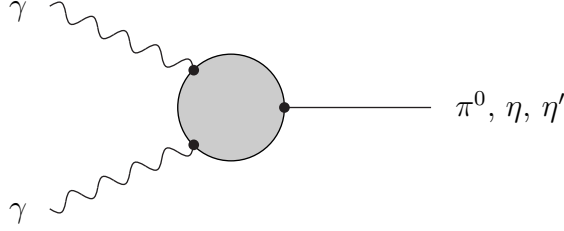


Figure 2: The realistic situation with more quark and gluon effects.

gluons and the reaction is more like in Fig. 2, where the shaded area includes different effects from quarks and gluons. If these effects are taken into account other terms come in which are added to the point-like Lagrangian. The new terms all have to fulfill the condition $\partial_\mu S^\mu = 0$, which means that they don't add anything to the four-divergence and the total Lagrangian still meets the requirement of the anomaly condition. But these new quark and gluon terms are very difficult to handle so they are omitted and their effects are only introduced as a form-factor. That is, a factor is multiplied to the vertex which takes into account all the effects that the extra terms would add. But since these effects are not completely known, the shape of the form-factor is uncertain. Still, there exist some constraints on it.

2.1 Constraints on the Form-factors

The form-factor connects three particles and therefore depends on three variables, the momentum-squared of the photons and the pseudo scalar. However, since we work under the approximation that the quark-mass is zero, the pseudo scalar will also become massless. Unlike the photons, which can be virtual, this will mean that q_{PS}^2 will always be zero and we set

$$F(k_1^2, k_2^2, 0) = F(k_1^2, k_2^2),$$

where k_1 and k_2 are the four-momenta of the two photons.

It would be very hard to find a form-factor that describes this transition well if one didn't have any constraints on how it should behave. Luckily, it is possible to calculate, directly from QCD, how it looks in certain limits. There are actually four different requirements on the shape of the form-factor. Three which are demands from QCD-calculations and one of a more argumentative nature.

The first limit in which the form-factor is known is when $k_1^2 = k_2^2 = 0$, that is, when the two photons are real. Then the transition can be compared to other processes like $\pi^+ \rightarrow \mu^+ \nu_\mu$, and it is actually in this limit that the Lagrangian is defined and F_π is set. So here, by definition, all quark and gluon effects are included in the pointlike Lagrangian and the form-factor must fulfill the relation

$$F(0, 0) = 1.$$

The next case where it is possible to calculate the result from QCD is when both photons are very much off shell and have the same virtuality, that is $k_1^2 = k_2^2 \ll 0$. In this case

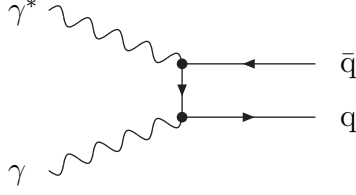


Figure 3: The high momentum implies that the quarks move parallel to each other.

one can use what is called the operator product expansion technique and calculate the matrix-element related to this transition up to order $1/k^2$. This gives the answer

$$F(k_1^2, k_2^2) = -\frac{8\pi^2 F_\pi^2}{N_c k^2}, \quad k_1^2 = k_2^2 = k^2 \ll 0,$$

where N_c is the number of colours in the Standard Model, which is three.

The third limit is when one of the photons is real and the other one very much off shell, e.g. $k_1^2 = 0$ and $k_2^2 \ll 0$. Which one is zero doesn't matter since the form-factor has to be symmetric in the two photons. In this case one can use that this is an exclusive process at high momentum transfer and the transition can be seen like in Fig. 3 where the quark and anti-quark that builds up the meson move parallel to each other. This simplifies the calculations and the answer from QCD is

$$F(0, k^2) = -\frac{C 8\pi^2 F_\pi^2}{N_c k^2}, \quad k_1^2 = 0, k_2^2 = k^2 \ll 0.$$

where C is a constant that is 1, 2 or 3 depending on further physical assumptions [4].

That $F(k_1^2, k_2^2)$ goes like $1/k^2$ in these two cases is very reliable. The next terms are of the order $1/k^4$ so they are obviously much smaller. The coefficients in front are a bit more uncertain though, since corrections to them are of order $\log(k^2)$ and that is not so small. This will be referred to in the next section.

The last constraint is not of the same form as the others. It is just that one believes that the quark and gluon effects which are not included in the pointlike treatment should somehow correspond to intermediate states with other mesons, like ρ . This idea comes among other things from the fact that the similar reaction $e^+e^- \rightarrow \gamma^* \rightarrow \pi^+\pi^-$ is very well explained in a picture with an intermediate state like $e^+e^- \rightarrow \gamma^* \rightarrow \rho \rightarrow \pi^+\pi^-$. This means that the shape of the form-factor should be such that it can be explained within the picture of an intermediate state vector meson. This is not absolutely certain since one doesn't really know the QCD-calculations, but there are some other theoretical arguments that point in this direction as well [5].

2.2 The Form-factors in this Article

It proves very hard to find a form-factor that satisfies these four constraints. Actually none of the factors we study in this article does that. We have chosen four different form-factors, each satisfying some of the constraints, but not all. Nevertheless, it is still possible to see how much the choice of form-factor influences different physical quantities.

The first form-factor is just $F(k_1^2, k_2^2) = 1$. That means no form-factor, and the reaction is seen as pointlike. This form-factor obviously satisfies the first constraint but not the others. This is no realistic form but it can be studied to see how much the introduction of a form-factor means.

The next form-factor is constructed to reproduce the experimental data that exist in this area. Experiments has been done with one photon real and the other off shell [6]. All our form-factors will be compared to these data in the next section. This form-factor is

$$F(k_1^2, k_2^2) = \frac{m_\rho^4}{(m_\rho^2 - k_1^2)(m_\rho^2 - k_2^2)},$$

where m_ρ is the mass of the ρ -meson. It satisfies the first and fourth requirement and with $F_\pi = 92.4 \text{ MeV}$ and $m_\rho = 770 \text{ MeV}$ it satisfies the third constraint within the uncertainty mentioned above.

The third form-factor we have made up ourselves to satisfy three of the four constraints and it looks like

$$F(k_1^2, k_2^2) = \frac{m_\rho^2}{(m_\rho^2 - k_1^2 - k_2^2)}.$$

It satisfies constraint one, two and three with the same comment as the last one, but not four, it can't be explained in terms of intermediate vector mesons.

The last one is also constructed to satisfy a specific requirement, but this time number two. It is

$$F(k_1^2, k_2^2) = \frac{m_\rho^4 - \frac{4\pi^2 F_\pi^2}{N_c} (k_1^2 + k_2^2)}{(m_\rho^2 - k_1^2)(m_\rho^2 - k_2^2)},$$

and it satisfies constraint one, two and four.

To sum up, the form-factors we are looking at in this article are:

$$\text{Form Factor 1 : } F(k_1^2, k_2^2) = 1$$

$$\text{Form Factor 2 : } F(k_1^2, k_2^2) = \frac{m_\rho^4}{(m_\rho^2 - k_1^2)(m_\rho^2 - k_2^2)}$$

$$\text{Form Factor 3 : } F(k_1^2, k_2^2) = \frac{m_\rho^2}{(m_\rho^2 - k_1^2 - k_2^2)}$$

$$\text{Form Factor 4 : } F(k_1^2, k_2^2) = \frac{m_\rho^4 - \frac{4\pi^2 F_\pi^2}{N_c} (k_1^2 + k_2^2)}{(m_\rho^2 - k_1^2)(m_\rho^2 - k_2^2)}$$

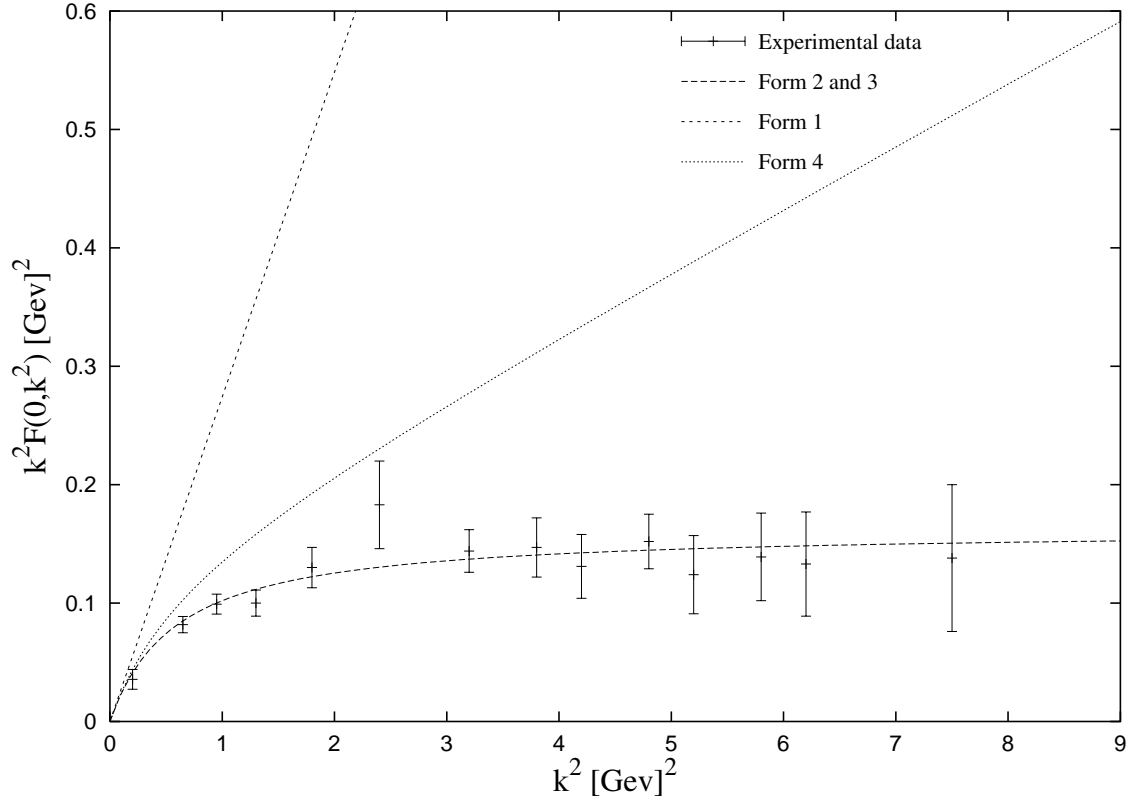


Figure 4: Comparison between our four form-factors and data from the CLEO collaboration.

2.3 Comparison with Experiment

Experiments with form-factors has been done by the CLEO collaboration [6]. They have studied the pion form-factor in the case that one of the photons is real and the other one is virtual. In this case our Form 2 and Form 3 have the same shape. In Fig. 4 the form-factors presented in the last section are compared with the data from the experiment. Their normalization of the form-factors is not the same as ours. Therefore our form-factors from the last section are multiplied with a factor

$$\sqrt{\frac{64\pi \Gamma(\pi^0 \rightarrow \gamma\gamma)}{(4\pi\alpha)^2 m_{\pi^0}^3}}.$$

It is easy to see that Form 1 and Form 4 do not satisfy the data as well as the other two. But still we will study the results from them to get a feeling for how much influence an incorrect form factor will have on various results.

3 Decay Rates

The decay rate of a particle is related to its lifetime. One version of Heisenbergs uncertainty relation can be written

$$\Delta E \Delta t \simeq \hbar, \quad (1)$$

where Δt can be seen as the lifetime of a particle. If a particle has a finite lifetime, Eq. (1) states that it must have an uncertainty in energy. This uncertainty is usually called the decay width, or the decay rate, of the particle.

In this section the decay rates of three processes, which include the meson-photon-photon vertex $\eta \rightarrow \gamma\gamma$, is calculated. The reason for choosing η is that an upcoming experiment, WASA at CELSIUS, Uppsala, is going to produce up to 10^{10} η -particles. Therefore, it is interesting to conclude whether they will be able to see the difference between the form-factors. We will present results for our four form-factors to see whether they can be distinguished in the experiment. But first we study π^0 decay to check our approximations.

3.1 $\pi^0 \rightarrow \gamma\gamma$

First we will study this process where π^0 decays. There is no dependence on form-factors since both photons are real, but it is still interesting to study it to check the different approximations we have made. The answer can be compared with the experimental lifetime of the pion and thus we have a measure of how well our calculations work.

3.1.1 The Amplitude

The process, as can be seen in Fig. 5, includes only the triangle vertex itself and no propagators. The triangle vertex is described by the Lagrangian

$$\mathcal{L} = -\frac{e^2}{4\sqrt{2}\pi^2 F_\pi} \partial_\mu A_\nu(x) A_\alpha(x) \partial_\beta \phi(x) \varepsilon^{\mu\nu\alpha\beta}. \quad (2)$$

Here $\phi(x)$ is the proper mixture of the meson fields,

$$\phi(x) = \frac{1}{\sqrt{2}}\pi^0(x) + \frac{1}{\sqrt{6}}\eta(x) + \frac{2}{\sqrt{3}}\eta'(x), \quad (3)$$

where e.g. the pion field is written as

$$\pi^0(x) = \int N_{\pi^0}(q) (e^{-iqx} a_q + e^{iqx} a_q^\dagger) d^3q. \quad (4)$$

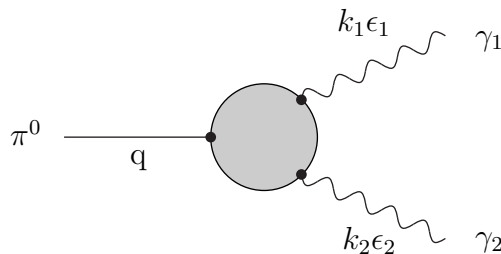


Figure 5: The decay of π^0 into two photons.

The operators a_q and a_q^\dagger annihilate and create, respectively, a pion with momentum q and $N_{\pi^0}(q)$ is a numerical factor which is taken care of by the Feynman rules. The other two meson fields can be written in the same way.

The photon field needs an extra index since it describes a vector particle and not a scalar. This is introduced as a polarization vector ϵ , which has four components. The photon field is then

$$A_\mu(x) = \int N_A(q) (\epsilon_\mu e^{-ikx} a_k + \epsilon_\mu^* e^{ikx} a_k^\dagger) d^3q. \quad (5)$$

In the process we are looking at one pion is annihilated and two photons are created. The corresponding terms are picked out from the field operators and used in the Lagrangian to get the Feynman amplitude for the vertex. This gives

$$A(\pi^0 \rightarrow \gamma\gamma) = \frac{e^2}{8\pi^2 F_\pi} \varepsilon^{\mu\nu\alpha\beta} q_\beta \epsilon_{1\nu}^* k_{1\mu} \epsilon_{2\alpha}^*. \quad (6)$$

But this is not the final answer. According to the Feynman rules an extra i should be added and furthermore, the photons are identical particles. This means that another term have to be added to the amplitude, in which the substitution $\gamma_1 \leftrightarrow \gamma_2$ is made. This gives the result

$$A(\pi^0 \rightarrow \gamma\gamma) = \frac{ie^2}{8\pi^2 F_\pi} \varepsilon^{\mu\nu\alpha\beta} q_\beta [\epsilon_{1\nu}^* k_{1\mu} \epsilon_{2\alpha}^* + \epsilon_{2\nu}^* k_{2\mu} \epsilon_{1\alpha}^*]. \quad (7)$$

3.1.2 The Matrix Element Squared

But to calculate the decay rate we need the amplitude squared, usually called the matrix element squared,

$$|M|^2 = |A|^2 = A A^*. \quad (8)$$

When this is calculated, one has to sum over all polarization states. This is taken care of by using the rule

$$\sum \epsilon_{1\nu} \epsilon_{1\tau}^* = -g_{\nu\tau}, \quad (9)$$

where the sum goes over the two polarization states of the photons and $g_{\nu\tau}$ is the metric tensor. Rules for the Levi-Civita tensor such as

$$\varepsilon^{\mu\nu\alpha\beta} \varepsilon_{\nu\alpha}^{\sigma\rho} = -2(g^{\mu\sigma} g^{\beta\rho} - g^{\mu\rho} g^{\sigma\beta}) \quad (10)$$

also have to be used.

The matrix element includes terms of scalar products of all the momenta in the process. These scalar products have to be calculated and put in. The result is

$$|M|^2(\pi^0 \rightarrow \gamma\gamma) = \frac{e^4}{2^6 \pi^4 F_\pi^2} m_{\pi^0}^4. \quad (11)$$

3.1.3 The decay rate

Now the matrix element squared should be connected to the decay rate. This is done using the general formula [7]

$$d\Gamma = \frac{(2\pi)^4}{2M} |M|^2 d\Phi_n, \quad (12)$$

where M is the mass of the decaying particle, n the number of particles in the final state and

$$d\Phi_n = \delta^4(\mathbf{P} - \sum_{i=1}^n \mathbf{p}_i) \prod_{i=1}^n \frac{d^3\vec{p}_i}{(2\pi)^3 2E_i} \quad (13)$$

In this case there are two degrees of freedom and the formula just gives

$$d\Gamma = \frac{|M|^2 |\mathbf{k}|}{32\pi^2 M^2} d\Omega \quad (14)$$

where $|\mathbf{k}|$ is the magnitude of either of the photons four momenta, equal for both.

In the case we are looking at $|\mathbf{k}| = m_\pi/2$, and since the two photons are identical and π^0 is a pseudo-scalar, $d\Omega = 2\pi$. The final result is then

$$\Gamma(\pi^0 \rightarrow \gamma\gamma) = \frac{\alpha^2 m_{\pi^0}^3}{2^6 \pi^3 F_\pi^2}$$

with $\alpha = e^2/4\pi$.

3.1.4 The Result

Putting in the numbers

$$F_\pi = 92.4 \text{ MeV} \quad \alpha = 1/137 \quad m_{\pi^0} = 134.98 \text{ MeV} \quad (15)$$

gives the numerical result

$$\Gamma(\pi^0 \rightarrow \gamma\gamma) = 7.734 \times 10^{-6} \text{ MeV} \quad (16)$$

Knowing how often the pion decays in this channel, it is possible to calculate its lifetime, τ .

$$\tau(\pi^0) = \frac{0.988}{\Gamma} = 127800 \text{ MeV}^{-1} = 8.41 \times 10^{-17} \text{ s}$$

Experiments give

$$\tau(\pi^0) = 8.4 \times 10^{-17} \text{ s}$$

so our approximations seem valid.

This is expected to be correct for the pion but wouldn't have been as exact for η and η' since they are more complicated. First of all the s quark is much heavier than the u and d quark, which make our approximations more severe for η and η' . Furthermore their mass is affected by gluon effects which we haven't included.

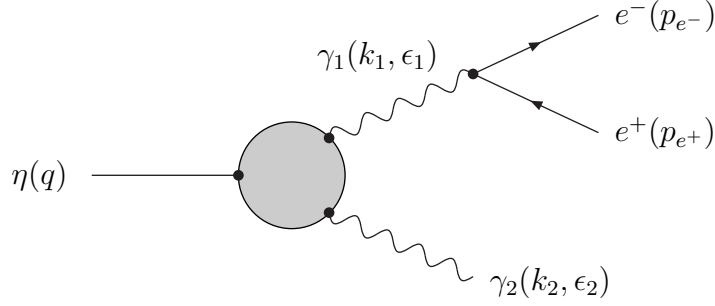


Figure 6: The decay of η into photon, electron and positron.

3.2 $\eta \rightarrow \gamma e^+e^-$ and $\eta \rightarrow \gamma \mu^+\mu^-$

The process with the electron and positron is described in Fig. 6 and it is the first case in which we can study the effects of the form factors. Here a new vertex is added which is described by the Lagrangian

$$\mathcal{L} = -e (\bar{e}\gamma^\mu e) A_\mu, \quad (17)$$

where \bar{e} and e are the positron and electron fields and γ stands for the γ -matrices. There is also a photon propagator, which according to the Feynman rules is described by $-i/k_1^2$ in this case. These two factors get multiplied to Eq. (2) which then leads to a new amplitude

$$A = -\frac{e^3}{8\sqrt{3}\pi^2 F_\pi} \varepsilon^{\mu\nu\alpha\beta} \frac{q_\beta}{k_1^2} [(\bar{e}\gamma_\alpha e)\epsilon_{1\nu}^* k_{1\mu} + (\bar{e}\gamma_\nu e)\epsilon_{1\alpha}^* k_{2\mu}]. \quad (18)$$

This is then squared, which e.g. includes working out traces of the γ -matrices. The result was checked with the program FORM. The matrix element squared is then used in the kinematics formula for three body decay, coming from Eq. (12),

$$d\Gamma = \frac{|M|^2}{(2\pi)^3 32M_{PS}^3} dm_{e^+e^-}^2 dm_{e^-\gamma}^2, \quad (19)$$

where $m_{e^+e^-}^2 = (p_{e^+} + p_{e^-})^2$ and $m_{e^-\gamma}^2 = (p_{e^-} + k_2)^2$ are the two degrees of freedom we have chosen. These are then integrated over, $dm_{e^-\gamma}^2$ analytically and $dm_{e^+e^-}^2$ using the Gaussian quadrature program DGAUSS. In the last integration different cuts on the lower limit are made to see if this gives more difference between the decay rates for different form-factors. The decay rate is then divided by

$$\Gamma^*(\eta \rightarrow \gamma\gamma) = 1.720 \times 10^{-4} \text{ MeV},$$

where $*$ means that it is our *theoretical* value of this decay rate. We use this one because of the arguments before that our approximations are not quite correct in the η and η' case. In this way, the same error should exist in both numerator and denominator so the ratio will be a more accurate number. The result is shown in Table 1, with numerical errors smaller than the last digit in the quoted values. The last line is the value without cut for $\eta \rightarrow \gamma \mu^+\mu^-$. We have used $M_\eta = 547.5 \text{ MeV}$.

cut (MeV^2)	Form 1	Form 2,3	Form 4
0	1.620×10^{-2}	1.666×10^{-2}	1.657×10^{-2}
2500	4.614×10^{-3}	5.071×10^{-3}	4.980×10^{-3}
10000	2.580×10^{-3}	3.000×10^{-3}	2.916×10^{-3}
22500	1.507×10^{-3}	1.869×10^{-3}	1.796×10^{-3}
40000	8.601×10^{-4}	1.150×10^{-3}	1.091×10^{-3}
62500	4.614×10^{-4}	6.748×10^{-4}	6.308×10^{-4}
90000	2.237×10^{-4}	3.636×10^{-4}	3.342×10^{-4}
122500	9.258×10^{-5}	1.705×10^{-4}	1.539×10^{-4}
160000	2.958×10^{-5}	6.322×10^{-5}	5.585×10^{-5}
202500	5.825×10^{-6}	1.488×10^{-5}	1.284×10^{-5}
250000	3.394×10^{-7}	1.077×10^{-6}	9.050×10^{-7}
$\gamma\mu^+\mu^-$	5.506×10^{-4}	7.744×10^{-4}	7.284×10^{-4}

Table 1: Decay rate for $\eta \rightarrow \gamma e^+e^-$, normalized to $\Gamma(\eta \rightarrow \gamma\gamma)$.

3.2.1 Experimental Uncertainties

It is necessary here to get a feeling for how large the uncertainty will be in the forthcoming experiment. A first estimate of the error is \sqrt{N} , where N is the number of decaying particles. N is given by

$$N = N_0 \frac{\Gamma}{\Gamma_{\gamma\gamma}} \frac{\Gamma_{\gamma\gamma}}{\Gamma_0} = N_0 \frac{\Gamma}{\Gamma_{\gamma\gamma}} BR(\eta \rightarrow \gamma\gamma), \quad (20)$$

where Γ_0 is the total decay rate and $\Gamma/\Gamma_{\gamma\gamma}$ the number given in the table. From this one can calculate the uncertainty on the normalized decay rate,

$$\frac{\Gamma}{\Gamma_{\gamma\gamma}} \pm \sqrt{\frac{\Gamma/\Gamma_{\gamma\gamma}}{BR(\eta \rightarrow \gamma\gamma) N_0}} \quad (21)$$

Without any cut and with $N_0 = 10^{10}$ and

$$BR(\eta \rightarrow \gamma\gamma) = 0.39,$$

this gives an uncertainty $\sigma \approx 10^{-6}$. So it should be possible to discern the different form-factors here.

But then a cut is introduced to see whether the difference between the form-factors will increase. For the cut on $160000 MeV^2$, the difference between the form-factors is quite sizeable. From Eq. (21) one sees that $\sigma \approx 10^{-7}$ in this case, which means that it should still be possible to distinguish between the three different form-factors with a high cut in the experiment. The reaction $\eta \rightarrow \gamma \mu^+\mu^-$ gives the same result.

It remains to check whether it is possible to see the difference between Form 2 and 3 in some other decay.

3.3 $\eta \rightarrow \mu^+\mu^- e^+e^-$

As one can see in Fig. 7, one new vertex and one new propagator is added to the last reaction. This leads to an amplitude

$$A = -\frac{ie^4}{8\sqrt{3}\pi^2 F_\pi} \epsilon^{\mu\nu\alpha\beta} \frac{q_\beta}{k_1^2 k_2^2} [(\bar{e}\gamma_\alpha e)k_{1\mu}(\bar{\mu}\gamma_\nu \mu) + (\bar{e}\gamma_\nu e)k_{2\mu}(\bar{\mu}\gamma_\alpha \mu)]. \quad (22)$$

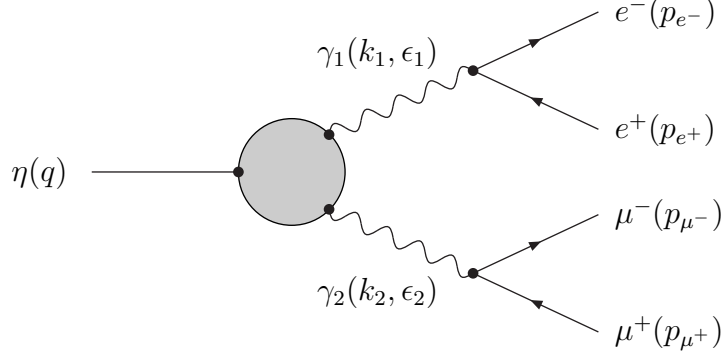


Figure 7: The decay of η into muon, anti-muon, electron and positron.

Calculating the corresponding matrix element squared includes working out the Dirac traces and once again the result is checked with FORM. The matrix element is then inserted in the formula for the four body decay rate, which has five degrees of freedom,

$$d\Gamma = \frac{|M|^2 |\vec{k}_1| |\vec{p}_e^*| |\vec{p}_\mu^{**}|}{(2\pi)^6 64 M^2 m_1 m_2} d(\cos \theta_1^*) d(\cos \theta_2^{**}) d\phi_2^{**} dm_1^2 dm_2^2, \quad (23)$$

where $m_1 = \sqrt{(p_{e+} + p_{e-})^2}$, $m_2 = \sqrt{(p_{\mu+} + p_{\mu-})^2}$ and $*(**)$ indicates that the quantity should be calculated in the rest frame of $\gamma_1(\gamma_2)$. These five degrees of freedom are again integrated over, this time the angle integrations are done analytically and the other two with DGAUSS. This leads to different results for the form-factors according to Table 2. Once again cuts are made, this time we impose a lower limit on m_1^2 , to see if this enhances the difference between the factors. For the lowest cut, 625 MeV^2 , the

cut (MeV^2)	Form 1	Form 2	Form 3	Form 4
0	3.99×10^{-6}	5.61×10^{-6}	5.62×10^{-6}	5.28×10^{-6}
625	1.39×10^{-6}	1.96×10^{-6}	1.97×10^{-6}	1.84×10^{-6}
2500	8.26×10^{-7}	1.16×10^{-6}	1.17×10^{-6}	1.09×10^{-6}
5625	5.21×10^{-7}	7.37×10^{-7}	7.44×10^{-7}	6.92×10^{-7}
10000	3.29×10^{-7}	4.68×10^{-7}	4.74×10^{-7}	4.39×10^{-7}
15625	2.03×10^{-7}	2.91×10^{-7}	2.96×10^{-7}	2.73×10^{-7}
22500	1.20×10^{-7}	1.74×10^{-7}	1.77×10^{-7}	1.63×10^{-7}
30625	6.64×10^{-8}	9.79×10^{-8}	9.99×10^{-8}	9.12×10^{-8}
40000	3.36×10^{-8}	5.04×10^{-8}	5.16×10^{-8}	4.68×10^{-8}
50625	1.49×10^{-8}	2.28×10^{-8}	2.34×10^{-8}	2.11×10^{-8}
62500	5.36×10^{-9}	8.46×10^{-9}	8.70×10^{-9}	7.78×10^{-9}
75625	1.37×10^{-9}	2.22×10^{-9}	2.29×10^{-9}	2.03×10^{-9}
90000	1.68×10^{-10}	2.82×10^{-10}	2.92×10^{-10}	2.57×10^{-10}

Table 2: Decay rate for $\eta \rightarrow \mu^+ \mu^- e^+ e^-$, normalized to $\Gamma(\eta \rightarrow \gamma \gamma)$.

uncertainty calculated from Eq. (21) is $\sigma \approx 10^{-8}$. Then it is possible to distinguish Form 1 and Form 4 from the others. For a higher cut, like 30625 MeV^2 , the error should

be $\sigma \approx 5 \times 10^{-9}$. It still is not possible to see the difference between Form 2 and Form 3.

3.4 $\eta \rightarrow e^+ e^- e^+ e^-$

The last decay we will study is the one depicted in Fig. 8. Kinematically, it is the same as the last one but the amplitude gets more complicated. A start is to take the amplitude from the last case, Eq. (22) and change μ to e_2 . This gives

$$A = -\frac{ie^4}{8\sqrt{3}\pi^2 F_\pi} \varepsilon^{\mu\nu\alpha\beta} \frac{q_\beta}{k_1^2 k_2^2} [(\bar{e}_1 \gamma_\alpha e_1) k_{1\mu} (\bar{e}_2 \gamma_\nu e_2) + (\bar{e}_1 \gamma_\nu e_1) k_{2\mu} (\bar{e}_2 \gamma_\alpha e_2)]. \quad (24)$$

But this isn't enough, because here we once again have identical particles. Two pairs of two identical particles give four diagrams, which can be divided into pairs which give equal results. The diagram in Fig. 8 represents one of the pairs and Fig. 9 represents the other pair. Both of these diagrams have to be taken into account and according to the Pauli principle they come in with different signs. Furthermore, this process is second order and this implies, according to the Feynman rules, an extra factor of $1/2$. Finally, the two pairs don't have the same propagators. In the first case they are

$$\begin{aligned} k_1 &= p_{e_1^+} + p_{e_1^-} \\ k_2 &= p_{e_2^+} + p_{e_2^-} \end{aligned}$$

but in the second case the propagators are

$$\begin{aligned} k_3 &= p_{e_1^+} + p_{e_2^-} \\ k_4 &= p_{e_2^+} + p_{e_1^-}. \end{aligned}$$

This gives an amplitude

$$A(\eta \rightarrow e^+ e^- e^+ e^-) = -\frac{ie^4}{8\sqrt{3}\pi^2 F_\pi} \varepsilon^{\mu\nu\alpha\beta} q_\beta \times [A_1 - A_2] \quad (25)$$

with

$$A_1 = \frac{(\bar{e}_1 \gamma_\nu e_1) k_{1\mu} (\bar{e}_2 \gamma_\alpha e_2) + (\bar{e}_1 \gamma_\alpha e_1) k_{2\mu} (\bar{e}_2 \gamma_\nu e_2)}{k_1^2 k_2^2} \quad (26)$$

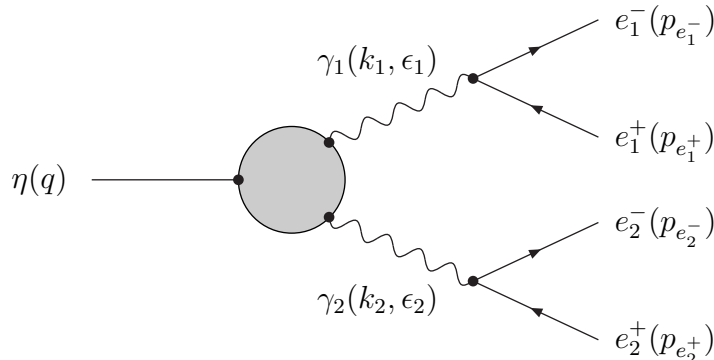


Figure 8: The decay of η into two electrons and two positrons.

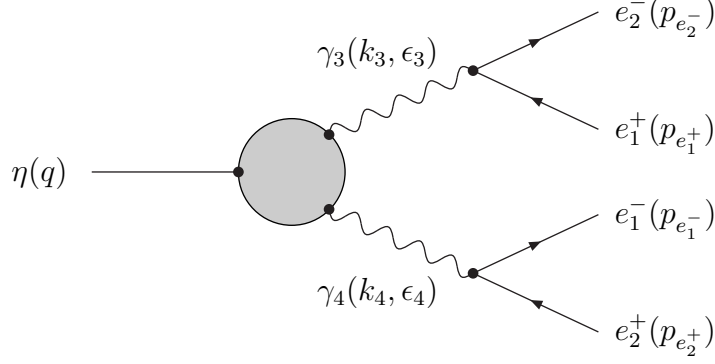


Figure 9: The other electron configuration.

and

$$A_2 = \frac{(\bar{e}_1 \gamma_\alpha e_2) k_{3\mu} (\bar{e}_2 \gamma_\nu e_1) + (\bar{e}_1 \gamma_\nu e_2) k_{4\mu} (\bar{e}_2 \gamma_\alpha e_1)}{k_3^2 k_4^2}. \quad (27)$$

This amplitude is then squared, using FORM, and put into Eq. (23), where an extra factor 1/4 is added since there are identical particles in the final state, to get the decay rate. The five degrees of freedom are integrated over using the Monte Carlo integration program VEGAS. Cuts are made on the low limit of k_1^2 , k_2^2 , k_3^2 and k_4^2 , and the result is presented in Table 3. The errors in parantheses are the errors quoted from VEGAS. The errors on the numbers without parantheses is maximum one in the last digit.

cut (MeV^2)	Form 1	Form 2	Form 3	Form 4
0	$6.40(2) \times 10^{-5}$	$6.73(2) \times 10^{-5}$	$6.71(2) \times 10^{-5}$	$6.64(2) \times 10^{-5}$
625	9.93×10^{-6}	1.10×10^{-5}	1.10×10^{-5}	1.08×10^{-5}
2500	3.83×10^{-6}	4.40×10^{-6}	4.41×10^{-6}	4.29×10^{-6}
5625	1.57×10^{-6}	1.86×10^{-6}	1.86×10^{-6}	1.80×10^{-6}
10000	6.07×10^{-7}	7.42×10^{-7}	7.46×10^{-7}	7.15×10^{-7}
15625	2.07×10^{-7}	2.63×10^{-7}	2.64×10^{-7}	2.51×10^{-7}
22500	5.80×10^{-8}	7.65×10^{-8}	7.73×10^{-8}	7.28×10^{-8}
30625	1.24×10^{-8}	1.73×10^{-8}	1.76×10^{-8}	1.63×10^{-8}
40000	1.86×10^{-9}	2.74×10^{-9}	2.79×10^{-9}	2.56×10^{-9}
50625	1.40×10^{-10}	2.19×10^{-10}	2.25×10^{-10}	2.01×10^{-10}
62500	1.74×10^{-12}	2.84×10^{-12}	2.96×10^{-12}	2.61×10^{-12}

Table 3: Decay rate for $\eta \rightarrow e^+ e^- e^+ e^-$, normalized to $\Gamma(\eta \rightarrow \gamma \gamma)$.

The difference between Form 2 and 3 is very small until the cut is 10000 MeV^2 . According to Eq. (21), the uncertainty here is $\sigma \approx 10^{-8}$, so it is not possible to see the difference here. For the highest cut the distinction is larger but the experimental uncertainty is up to the size of the value itself. So, unfortunately, it seems not to be possible to choose between form-factor 2 and 3 from decay experiments with this kind of precision. In the next section we will see if it is possible in collision experiments like $e^+ e^- \rightarrow e^+ e^- PS$, where PS is π^0 , η or η' .

4 Cross Sections

The cross section for a reaction is related to the probability for it to happen. The name comes from the classical picture where the total cross section for e.g. $p\bar{p}$ scattering is the area in which both particles have to be when they pass each other for a reaction to happen. The cross section for e.g. $p\bar{p} \rightarrow \pi^+\pi^-$ is then this area times the probability that precisely $\pi^+\pi^-$ is in the final state and nothing else.

The process $e^+e^- \rightarrow PS e^+e^-$, where PS is π^0 , η or η' , includes a meson-photon vertex. Therefore this is another opportunity to study the effects different form-factors will have. We will calculate the cross section for all three processes with our four different form-factors to see whether the difference will be larger here, possibly large enough to distinguish between Form 2 and 3.

Experimentally, these cross sections can be studied both at CESR, US, and at DAΦNE, Italy. At Cornell they are studied at CLEO with a center of mass energy $E_{CM} = 10.58 \text{ GeV}$ and in Italy at KLOE with $E_{CM} = 1.0192 \text{ GeV}$. We will look at both these energies in our calculations.

4.1 The Matrix Element

Irrespective of the pseudo-scalar created, two diagrams contribute to the process, depicted in Fig. 10 and Fig. 11. As seen, the process includes the same vertices and propagators as the earlier treated process $\eta \rightarrow e^+e^- e^+e^-$. Then, for reasons of crossing symmetry, the matrix element should also look the same, with a different numerical factor for π^0 and η' . But not exactly the same. The creation of one of the electron-positron pairs before corresponds to annihilation of a positron-electron pair now. This taken into account, the amplitude is

$$A(e^+e^- \rightarrow PS e^+e^-) = -\frac{ie^4}{C\pi^2 F_\pi} \varepsilon^{\mu\nu\alpha\beta} q_\beta \times [A_1 - A_2] \quad (28)$$

with

$$A_1 = \frac{(\bar{e}_1 \gamma_\nu e_1) k_{1\mu} (\bar{e}_2 \gamma_\alpha e_2) + (\bar{e}_1 \gamma_\alpha e_1) k_{2\mu} (\bar{e}_2 \gamma_\nu e_2)}{k_1^2 k_2^2}$$

$$A_2 = \frac{(\bar{e}_1 \gamma_\alpha e_2) k_{3\mu} (\bar{e}_2 \gamma_\nu e_1) + (\bar{e}_1 \gamma_\nu e_2) k_{4\mu} (\bar{e}_2 \gamma_\alpha e_1)}{k_3^2 k_4^2}$$

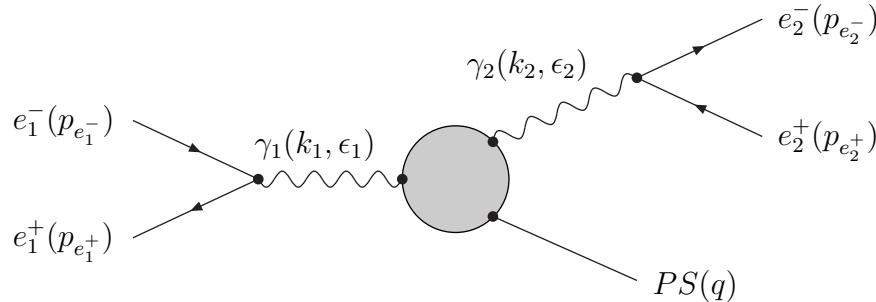


Figure 10: Diagram contributing to the cross section for $e^+e^- \rightarrow PS e^+e^-$.

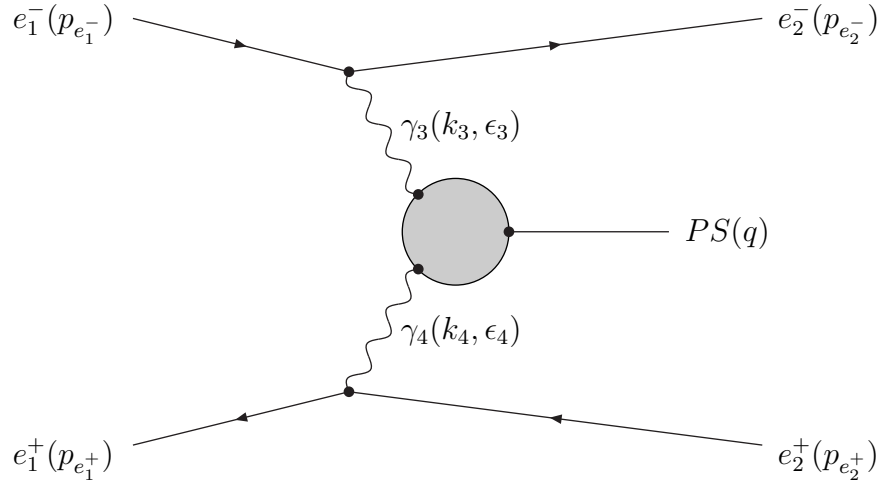


Figure 11: Second diagram contributing to the cross section for $e^+e^- \rightarrow PS e^+e^-$.

and

$$C = \begin{cases} 8 & \text{for } \pi^0 \\ 8\sqrt{3} & \text{for } \eta \\ 4\sqrt{3/2} & \text{for } \eta' \end{cases}$$

where the difference from the earlier case lies in which part of the electron and positron fields that are used. In the calculations we have used an effective C for η and η' , which reproduces the correct decay rates for them, $\Gamma(\eta \rightarrow \gamma\gamma) = 4.6 \times 10^{-4} \text{ MeV}$ and $\Gamma(\eta' \rightarrow \gamma\gamma) = 4.27 \times 10^{-3} \text{ MeV}$.

The amplitude is then squared and the result is the matrix element squared.

4.2 The Kinematics

The general formula for the cross section with three particles in the final state is [7]

$$d\sigma = \frac{(2\pi)^4 |M|^2 d\Phi_3}{4\sqrt{(\mathbf{p}_1 \cdot \mathbf{p}_2)^2 - m_1^2 m_2^2}}, \quad (29)$$

with

$$d\Phi_3 = \delta^4(\mathbf{p}_1 + \mathbf{p}_2 - \mathbf{p}_3 - \mathbf{p}_4 - \mathbf{p}_5) \frac{d^3\vec{p}_3}{(2\pi)^3 2E_3} \frac{d^3\vec{p}_4}{(2\pi)^3 2E_4} \frac{d^3\vec{p}_5}{(2\pi)^3 2E_5}$$

where \mathbf{p}_1 and \mathbf{p}_2 are the four momenta of the incoming particles and \mathbf{p}_3 , \mathbf{p}_4 and \mathbf{p}_5 are the momenta of the outgoing particles. In this case $d\Phi_3$ can be rewritten as

$$d\Phi_3 = \frac{|\vec{p}_{e_2^+}^*| d\Omega_{e_2^+}^* |\vec{p}_{e_2^-}| d\Omega_{e_2^-} dm_{PS e_2^+}^2}{16(2\pi)^9 m_{PS e_2^+} E_{CM}}, \quad (30)$$

where $m_{PS e_2^+} = \sqrt{(q + p_{e_2^+})^2}$ and $*$ means that the quantity is calculated in the rest frame of e_2^+ and the meson. Furthermore, since the lab system, where we want to calculate our quantities, is the same as the E_{CM} system we have

$$\mathbf{p}_1 = \left(\frac{E_{CM}}{2}, 0, 0, \sqrt{\frac{E_{CM}^2}{4} - m_e^2} \right) \quad (31)$$

$$\mathbf{p}_2 = \left(\frac{E_{CM}}{2}, 0, 0, -\sqrt{\frac{E_{CM}^2}{4} - m_e^2} \right),$$

which implies

$$\sqrt{(\mathbf{p}_1 \cdot \mathbf{p}_2)^2 - m_1^2 m_2^2} = E_{CM} |\vec{p}_{in}|, \quad (32)$$

where p_{in} is either p_1 or p_2 .

4.3 The Result

The z-axis is set by the incoming particles, but one can rotate freely around it. This means that one of the angles in $d\Omega_{e_2^-}$ becomes just 2π . Furthermore, a factor $1/4$ is added since one has to take the average over incoming spins. Then there are four degrees of freedom left and the expression for the cross section is

$$d\sigma = \frac{|\vec{p}_{e_2^+}^*| |\vec{p}_{e_2^-}| |M|^2}{2^8 (2\pi)^4 m_{PSe_2^+} E_{CM}^2 |\vec{p}_{in}|} dm_{PSe_2^+}^2 d\Omega_{e_2^+}^* d\cos\theta_2. \quad (33)$$

The matrix element squared is made up of scalar products of the four vectors $p_{e_1^+}$, $p_{e_2^+}$, $p_{e_1^-}$ and $p_{e_2^-}$. Therefore one has to figure out how these vectors look in some common frame. This is done by expressing them in a frame where they are known and then rotating and boosting them to the lab frame.

Then everything is known and one can integrate to get the full cross section. This is again done by using VEGAS integration on all four degrees of freedom. Cuts are introduced, this time directly on the angle between the outgoing electron and positron and the z-axis. The lowest cut is constructed so that the electron and positron precisely go through the tracking system of the detectors.

The results, in pbarns, are presented in Table 4 to Table 9. The numerical errors are maximum one in the last digit.

We have used the following masses

$$m_{\pi^0} = 134.98 \text{ MeV} \quad m_\eta = 547.5 \text{ MeV} \quad m_{\eta'} = 957.8 \text{ MeV},$$

cut ($ \cos\theta <$)	Form 1	Form 2	Form 3	Form 4
0.9	2.41	2.09	1.94	1.63
0.8	1.38	1.33	1.21	0.919
0.6	0.596	0.690	0.627	0.409
0.4	0.266	0.355	0.328	0.191

Table 4: Cross section for $e^+e^- \rightarrow \pi^0 e^+e^-$ with $E_{CM} = 1.019 \text{ GeV}$ and extra cut.

cut ($ \cos\theta <$)	Form 1	Form 2	Form 3	Form 4
0.93	4.43	6.83×10^{-4}	6.20×10^{-3}	3.56×10^{-2}
0.8	1.76	3.69×10^{-5}	5.25×10^{-4}	2.05×10^{-2}
0.6	0.762	1.23×10^{-5}	8.58×10^{-5}	1.32×10^{-2}
0.4	0.355	6.85×10^{-6}	2.39×10^{-5}	8.04×10^{-3}

Table 5: Cross section for $e^+e^- \rightarrow \pi^0 e^+e^-$ with $E_{CM} = 10.58 \text{ GeV}$ and extra cut.

cut ($ \cos\theta <$)	Form 1	Form 2	Form 3	Form 4
0.9	1.26	0.974	0.963	0.871
0.8	0.694	0.557	0.548	0.457
0.6	0.291	0.260	0.255	0.186
0.4	0.123	0.126	0.123	0.0800

Table 6: Cross section for $e^+e^- \rightarrow \eta e^+e^-$ with $E_{CM} = 1.019 \text{ GeV}$

cut ($ \cos\theta <$)	Form 1	Form 2	Form 3	Form 4
0.93	3.90	6.06×10^{-4}	5.48×10^{-3}	3.15×10^{-2}
0.8	1.55	3.27×10^{-5}	4.65×10^{-4}	1.81×10^{-2}
0.6	0.673	1.09×10^{-5}	7.63×10^{-5}	1.17×10^{-2}
0.4	0.314	6.05×10^{-6}	2.12×10^{-5}	7.10×10^{-3}

Table 7: Cross section for $e^+e^- \rightarrow \eta e^+e^-$ with $E_{CM} = 10.58 \text{ GeV}$ and extra cut.

4.3.1 Additional Cuts

As stated earlier, some of the form-factors corresponds to a physical picture with intermediate mesons e.g. ρ . Therefore the mathematical expression of those factors are related to a meson propagator,

$$\frac{1}{k^2 - M^2}, \quad (34)$$

where k is the four momenta and M the mass of the meson. This is however only an approximation of the full propagator, which should include different higher order corrections, such as loops. This would have changed the propagator to

$$\frac{1}{k^2 - M^2 - \Sigma}, \quad (35)$$

where Σ is a complex quantity related to the decay rate of the propagating meson.

Using this approximation introduces problems when $k^2 = M^2$, which will happen in some cases with the energies above. In the case with the high energy, $E_{CM} = 10.58 \text{ GeV}$, the problem arises with all three of the particles. This is solved by introducing a new cut. All events in which k_1^2 , k_2^2 , k_3^2 or k_4^2 is in the range $(M_\rho - 300 \text{ MeV})^2 \rightarrow (M_\rho + 300 \text{ MeV})^2$ are not counted in the cross section. The reason for choosing 300 MeV is that it is twice the decay width of the ρ . A good approximation for Σ is $iM_\rho\Gamma_\rho$, which means that when

cut ($ \cos\theta <$)	Form 1	Form 2	Form 3	Form 4
0.9	0.205	0.183	0.183	0.187
0.8	0.114	0.100	0.100	0.102
0.6	0.0457	0.0391	0.0392	0.0399
0.4	0.0172	0.0145	0.0146	0.0148

Table 8: Cross section for $e^+e^- \rightarrow \eta' e^+e^-$ with $E_{CM} = 1.019 \text{ GeV}$

cut ($ \cos\theta <$)	Form 1	Form 2	Form 3	Form 4
0.93	6.61	1.05×10^{-3}	9.38×10^{-3}	5.38×10^{-2}
0.8	2.65	5.65×10^{-5}	8.02×10^{-4}	3.09×10^{-2}
0.6	1.15	1.87×10^{-5}	1.32×10^{-4}	2.00×10^{-2}
0.4	0.536	1.03×10^{-5}	3.65×10^{-5}	1.21×10^{-2}

Table 9: Cross section for $e^+e^- \rightarrow \eta' e^+e^-$ with $E_{CM} = 10.58 \text{ GeV}$ and extra cut.

$q = M_\rho \pm 2\Gamma_\rho$, the absolute value of the term we have neglected can at most be one fourth of q^2 , and therefore should not make a large difference.

The same thing happens with the low energy and the pion. But this time it is not possible to use the same cut as last time, since all our events lie in that region. We solve this by cutting in a more narrow interval, $M_\rho \pm 200 \text{ MeV}$. Then the neglected term can be up to half the size of the terms left but that will have to do.

Experimentally, it is all right to make a more narrow cut in the low energy case. A narrow cut means that a small error in the measurement of the energy will make much difference, but this is compensated by the fact that low energy means better resolution, experimentally.

4.3.2 Experimental Uncertainties

Once again it is interesting to calculate the uncertainties in the experiments. The number of events is in this case given by the formula

$$N = L \sigma \Delta t, \quad (36)$$

where L is the luminosity of the experiment and Δt the running time. In both experiments the standard luminosity should be $L = 5 \times 10^{32} \text{ cm}^{-2} \text{ s}^{-1}$ and we will calculate with one year of running time, $\Delta t = 10^7 \text{ s}$.

As mentioned before, a first estimate of the uncertainty is $\pm\sqrt{N}$, where N is the number of events. From this one can get

$$\sigma \pm \sqrt{\frac{\sigma}{L \Delta t}} \quad (37)$$

which is the result we use.

4.3.3 Conclusions

Just as in the decay rates it is possible to distinguish between Form 1 and 4 in all of these experiments. However, here the difference is large between Form 2 and 3 in some cases as well.

In the high energy experiment it should actually be possible to discern all four form-factors for all three particles. For e.g. η with the cut $|\cos\theta| < 0.93$, the results with errors are

$$\begin{array}{ll}
\text{Form 1} & (3.90 \pm 0.03) \\
\text{Form 2} & (6 \pm 3) \times 10^{-4} \\
\text{Form 3} & (5 \pm 1) \times 10^{-3} \\
\text{Form 4} & (3.2 \pm 0.3) \times 10^{-2}
\end{array} \tag{38}$$

In the low energy experiments it is more difficult. There it is only in the case with the pion that it should be possible to distinguish between all four. The results, with cut $|\cos\theta| < 0.9$ are

$$\begin{array}{ll}
\text{Form 1} & (2.41 \pm 0.02) \\
\text{Form 2} & (2.09 \pm 0.02) \\
\text{Form 3} & (1.94 \pm 0.02) \\
\text{Form 4} & (1.63 \pm 0.02)
\end{array} \tag{39}$$

On the other hand, the difference is visible for all the four different cuts in this case.

The above numbers are calculated with the luminosity mentioned above and a typical year, which totals to an integrated luminosity of 5000 pb^{-1} .

5 The Muon Anomalous Magnetic Moment

A magnetic moment is associated with a rotating charged body. Classically this magnetic moment μ is related to the angular momentum l of the rotation through

$$\mu = \frac{q}{2m} l, \quad (40)$$

where q is the charge and m is the mass of the body. But particles also have intrinsic angular momentum, spin. This also gives rise to a magnetic moment according to

$$\mu_s = g_s \frac{q}{2m} s, \quad (41)$$

where s is the spin angular momentum vector and q and m is the charge and the mass of the particle. g_s , known as the gyromagnetic ratio, is just a constant which, according to Dirac theory, is exactly equal to 2 for electrons and muons.

However, in Quantum Field Theory, which treats particles as quantized fields as mentioned in the introduction, this is no longer true. Fig. 12 depicts the lowest order diagram for the interaction between a muon and a magnetic field, which gives $g_s = 2$.

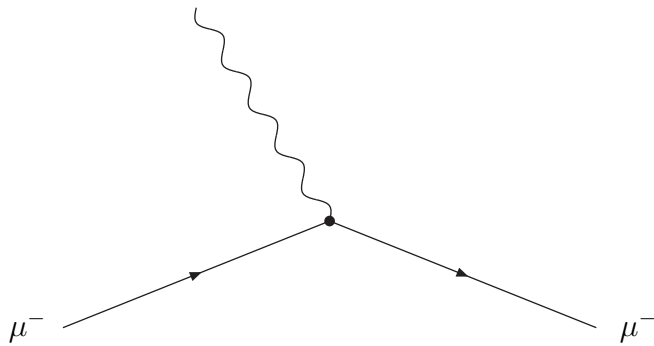


Figure 12: Lowest order diagram for muon scattering by a magnetic field.

But then there are higher order corrections, which will change the amplitude for the interaction between the muon and the magnetic field. This can be taken care of by changing the value of the gyromagnetic ratio by a small amount. To study these corrections one defines the anomalous magnetic moment, a_μ , as

$$a_\mu = \frac{1}{2} (g_s - 2). \quad (42)$$

This will then be a measure of how large the higher order corrections from Quantum Field Theory are. At present the theoretical standard model estimate for a_μ is [4, 8, 9]

$$a_\mu(th) = 11659178(7) \times 10^{-10},$$

where the estimated error is in parentheses. a_μ gets contributions from five different types of diagrams.

1. Pure QED contributions are the largest corrections. They consist e.g. of extra photon propagators or quark- and lepton loops, see Fig. 13.

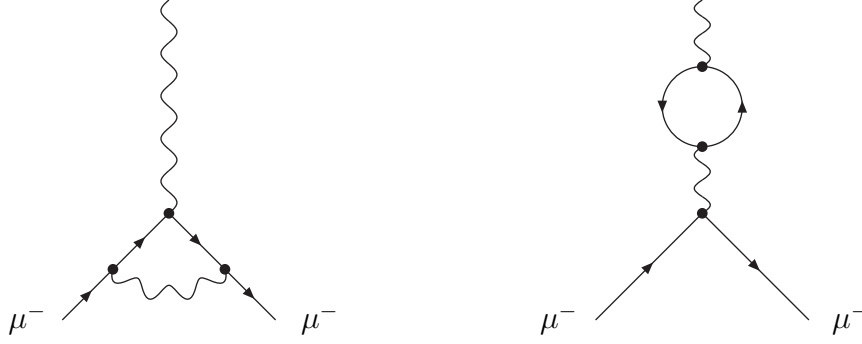


Figure 13: Higher order QED diagrams for muon scattering by a magnetic field.

2. Hadronic vacuum polarization, which means that all kinds of hadron effects are added to the photons, e.g. quark-loops or intermediate mesons.
3. Higher order hadronic vacuum polarization effects, which means even more hadron effects.
4. Hadronic light-by-light scattering contributions. These are more complicated splittings and loops in the photon from the magnetic field. The dominant diagram is depicted in Fig. 14.
5. Electroweak contributions, which means that Z^0 - and W^\pm -propagators are added in different ways.

The piece that is studied in this paper is the one depicted in Fig. 14, since it includes two meson-photon-photon vertices and therefore also depends on the form-factors. We will calculate the contribution from this process to the anomalous magnetic moment for our form-factors 2,3 and 4 and compare the results.

A running experiment at Brookhaven National Laboratory measures the anomalous magnetic moment for the muon. In the future they hope to get an accuracy around $\pm 4 \times 10^{-10}$, improving by a factor more than twenty the previous experimental determination at CERN. Therefore, it is important that the theoretical uncertainties are lowered

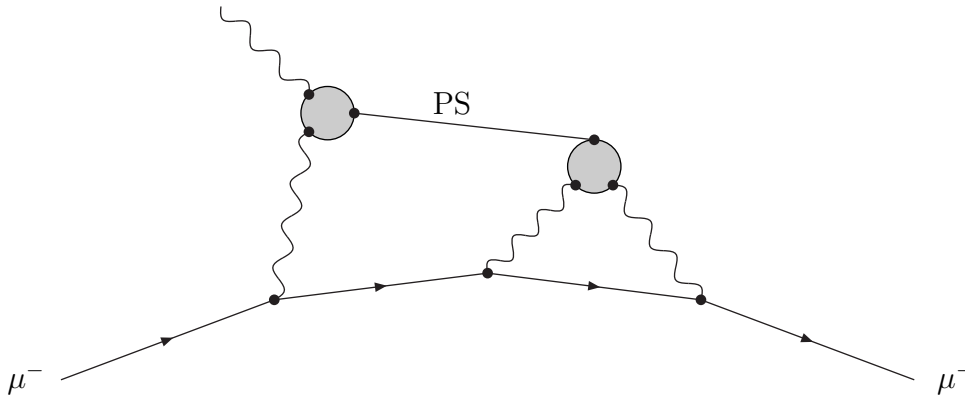


Figure 14: The dominant light-by-light contribution to the muon magnetic moment.

to the same order as the aimed BNL uncertainty. Then the measurement can become a precision test of the quantum corrections of the electroweak sector of the Standard Model. Even more, with the same low theoretical and experimental uncertainties, and when combined with other high precision results, a_μ could become an excellent probe of physics beyond the Standard Model.

5.1 The Result

All of the hadronic light-by-light contributions can be depicted as in Fig. 15, where the shaded blob includes all kinds of hadronic effects. The numbering in the figure corresponds to one of six permutations, due to the photons being identical particles. The amplitude for this process is [8]

$$\begin{aligned}
A &= |e|^7 A_\beta \int \frac{d^4 p_1}{(2\pi)^4} \int \frac{d^4 p_2}{(2\pi)^4} \frac{1}{q^2 p_1^2 p_2^2 (p_4^2 - m^2)(p_5^2 - m^2)} \\
&\quad \times \Pi^{\rho\nu\alpha\beta}(p_1, p_2, p_3) \bar{u}(p') \gamma_\alpha (\not{p}_4 + m) \gamma_\nu (\not{p}_5 + m) \gamma_\rho u(p) \\
&\quad + \text{five more permutations,}
\end{aligned} \tag{43}$$

where $\Pi^{\rho\nu\alpha\beta}$, called the four-point function, describes the shaded blob. In our case, $\Pi^{\rho\nu\alpha\beta}$ is just the product of the vertices and propagators corresponding to Fig. 14. For low momentum transfer, this amplitude can be expanded in a Taylor series in $(p - p')$. The linear term is then, with the momentum transfer set to zero, by definition the anomalous magnetic moment. We calculate the pseudo-scalar light-by-light contribution to this term for form-factor 2, 3 and 4. In doing that, the integrations in Eq. (43) should go from zero to infinity. But it is interesting to see from which energy-regions the contributions come. Therefore, we introduce a cut on the upper limit. This cut is then raised until the result converges to some number, which means that a_μ^{PS} has been saturated. The result is presented in Table 10 when $PS = \pi^0$, Table 11 when $PS = \eta$ and Table 12 when $PS = \eta'$. The numbers in parentheses are the errors quoted by VEGAS. The contributions from the three pseudo scalar mesons should then be added to get the final value of a_μ^{PS} . The

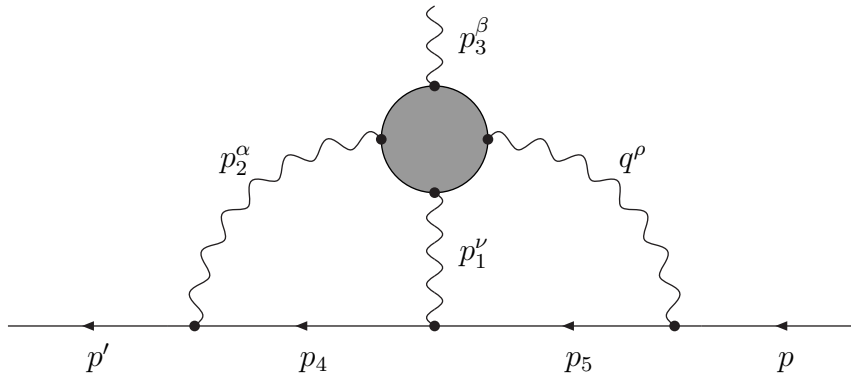


Figure 15: Hadronic light-by-light contribution to a_μ .

cut (GeV)	Form 2 ($\times 10^{-10}$)	Form 3 ($\times 10^{-10}$)	Form 4 ($\times 10^{-10}$)
0.4	-2.683(2)	-2.707(2)	-2.821(2)
0.5	-3.440(3)	-3.449(3)	-3.683(3)
0.7	-4.448(5)	-4.622(5)	-4.936(5)
1.0	-5.152(7)	-5.538(8)	-5.972(8)
2.0	-5.60(1)	-6.43(1)	-6.96(1)
4.0	-5.64(1)	-6.67(2)	-7.21(2)
8.0	-5.63(1)	-6.74(2)	-7.27(2)
12.0	-5.63(1)	-6.70(2)	-7.25(2)

Table 10: a_μ^{PS} when $PS = \pi^0$.

cut (GeV)	Form 2 ($\times 10^{-10}$)	Form 3 ($\times 10^{-10}$)	Form 4 ($\times 10^{-10}$)
0.4	-0.4029(2)	-0.4071(2)	-0.4289(2)
0.5	-0.5819(3)	-0.5936(3)	-0.6353(3)
0.7	-0.8678(6)	-0.9088(6)	-0.9967(6)
1.0	-1.1058(9)	-1.211(1)	-1.357(1)
2.0	-1.281(1)	-1.545(2)	-1.768(2)
4.0	-1.301(2)	-1.647(3)	-1.900(3)
8.0	-1.302(2)	-1.670(3)	-1.937(3)
12.0	-1.301(2)	-1.676(4)	-1.943(3)

Table 11: a_μ^{PS} when $PS = \eta$.

result is

$$\begin{aligned}
\text{Form Factor 2} & -7.94 \times 10^{-10} \\
\text{Form Factor 3} & -9.73 \times 10^{-10} \\
\text{Form Factor 4} & -10.85 \times 10^{-10}
\end{aligned} \tag{44}$$

If nothing else were known of the form-factors, one would have to take the mean value of all these and an uncertainty that covered all of them. Then the final result would be

$$a_\mu^{PS} = -(9.51 \pm 1.6) \times 10^{-10}. \tag{45}$$

However, it looks like it is possible to exclude Form 4 already from the experiment mentioned in Section 2.3. Therefore, we take a mean value of Form 2 and 3, which gives

$$a_\mu^{PS} = -(8.83 \pm 0.9) \times 10^{-10}. \tag{46}$$

This is our final result for a_μ^{PS} and since it isn't possible to discern Form 2 and 3 yet, this must be the smallest possible uncertainty on this value. This can be compared with the result in reference [8]

$$a_\mu^{PS} = -(8.5 \pm 1.3) \times 10^{-10} \tag{47}$$

and [4]

$$a_\mu^{PS} = -(8.27 \pm 0.64) \times 10^{-10} \tag{48}$$

cut (GeV)	Form 2 ($\times 10^{-10}$)	Form 3 ($\times 10^{-10}$)	Form 4 ($\times 10^{-10}$)
0.4	-0.2595(1)	-0.2623(1)	-0.2770(1)
0.5	-0.3882(2)	-0.3964(2)	-0.4260(2)
0.7	-0.6113(4)	-0.6417(4)	-0.7102(4)
1.0	-0.8168(6)	-0.9008(6)	-1.0262(7)
2.0	-0.9874(9)	-1.219(1)	-1.443(1)
4.0	-1.008(1)	-1.324(2)	-1.597(2)
8.0	-1.010(1)	-1.351(2)	-1.645(2)
12.0	-1.009(1)	-1.353(2)	-1.654(3)

Table 12: a_μ^{PS} when $PS = \eta'$.

Even if neither Form 2 nor Form 3 satisfies all the physical demands on a form-factor, our result means that one can not use arguments from existing experiments to lower the uncertainty more than ours. To get better precision, experiments like the cross sections mentioned in Section 4 have to be done, which can better discern between different form-factors.

6 Summary

In this thesis we have been studying form-factors in meson-photon-photon transitions. In this kind of transitions the exact form of the form factors is not known and therefore different types are investigated. We have studied four different factors, which all satisfy some, but not all, of the constraints on form-factors coming from QCD. They are

$$\text{Form Factor 1 : } F(k_1^2, k_2^2) = 1$$

$$\text{Form Factor 2 : } F(k_1^2, k_2^2) = \frac{m_\rho^4}{(m_\rho^2 - k_1^2)(m_\rho^2 - k_2^2)}$$

$$\text{Form Factor 3 : } F(k_1^2, k_2^2) = \frac{m_\rho^2}{(m_\rho^2 - k_1^2 - k_2^2)}$$

$$\text{Form Factor 4 : } F(k_1^2, k_2^2) = \frac{m_\rho^4 - \frac{4\pi^2}{N_c} F_\pi^2 (k_1^2 + k_2^2)}{(m_\rho^2 - k_1^2)(m_\rho^2 - k_2^2)}$$

The idea is to calculate a set of physical quantities whose value depend on the choice of form-factor. This is done to see if it should be possible to distinguish between the four in experiment. Already in section 2, results from an experiment done by the CLEO collaboration were presented, which more or less rules out Form 1 and 4.

In section 3 the decay rates of processes involving $\eta \rightarrow \gamma\gamma$ are calculated. The results are compared with the expected uncertainty from an upcoming experiment WASA at CELSIUS, Uppsala. Here again it seems like they will be able to exclude Form 1 and 4 but not choose between Form 2 and 3.

In section 4 the cross section of three processes, which include a meson-photon-photon transition, are calculated. The results are again compared with estimated uncertainties, this time from experiments at CESR, US and at DAΦNE, Italy. It turns out that in this type of experiments it should be possible to make a more precise measurement of form-factors and possibly discern all four.

Finally, in section 5, we make some comments about how the present uncertainty around the choice of form-factor affects the value for the muon anomalous magnetic moment. When examining the pseudo-scalar part of the light-by-light contribution to a_μ , we can estimate the lowest possible error in the theoretical value by looking at how much it differs when using Form 2 and 3. Since no present experiment can discern between the two, the uncertainty must be at least large enough to cover both values. To get a better precision, experiments have to be done, which can better discern between different form-factors. This is important since the muon anomalous magnetic moment is one of the most precisely measured quantities in physics and furthermore can be a probe for physics beyond the Standard Model.

Acknowledgements

First, I would like to thank my supervisor, Johan Bijnens, for introducing me to this subject and for patiently answering all my questions around it. I would also like to thank all the people at the department who have helped me during this time, and my family and friends for their support.

References

- [1] H-U. Bengtsson, G. Gustafson and L. Gustafson, “Kvarken och universum”, Corona (Malmö, 1994).
- [2] Gordon Kane, “Modern Elementary Particle Physics”, Addison-Wesley (Massachusetts, 1993).
- [3] John F. Donoghue, Eugene Golowich, Barry R. Holstein, “Dynamics of the Standard Model”, Cambridge University Press (Cambridge, 1992).
- [4] M. Hayakawa and T. Kinoshita, Phys. Rev. D 57 (1998) 465.
- [5] J. J. Sakurai, “Currents and Mesons”, University of Chicago Press (Chicago, 1969).
- [6] CLEO Collaboration, Phys. Rev. D 57 (1998) 33.
- [7] Particle Data Group, C. Caso et al., Eur. Phys. J. C 3 (1998) 1.
- [8] J. Bijnens, E. Pallante and J. Prades, Nucl. Phys. B474 (1996) 379.
- [9] F. Jegerlehner, preprint hep-ph/9901386 (1999).